Available online at www.sciencedirect.com
ScienceDirect
Proceedings of the Combustion Institute 31 (2007) 775–782
Proceedings of the Combustion Institute
www.elsevier.com/locate/proci

A thermometry technique based on atomic lineshapes using diode laser LIF in flames

I.S. Burns *, J. Hult, G. Hartung, C.F. Kaminski

Department of Chemical Engineering, University of Cambridge, Pembroke Street, Cambridge CB2 3RA, UK

Abstract

We report on the development of a novel diode laser thermometry technique permitting temperature measurements in flames based on the fluorescence lineshapes of an atomic tracer species. The technique, which we term OLAF (one-line atomic fluorescence) requires only a single diode laser source for excitation, is simple to implement, and has excellent spatial resolution. Temperatures are deduced from the $5^2P_{1/2} \rightarrow 6^2S_{1/2}$ transition of atomic indium, the lineshape of which is highly sensitive to temperature changes at typical flame conditions. A rigorous validation is performed in a reference flame with comparisons to measurements by CARS and by Na-line reversal, and to numerical simulations.

Keywords: Diode laser; LIF; Thermometry; Atomic fluorescence; Pressure broadening

1. Introduction

The importance of spatially resolved temperature measurements to the study of combustion is widely acknowledged. Laser techniques are best-suited to this task, since they fulfil the requirements for high spatial and temporal resolution, and for non-intrusiveness [1]. A number of laser techniques have been developed, including, coherent anti-Stokes Raman scattering (CARS), two-line laser-induced fluorescence (LIF), and Rayleigh scattering; these techniques have been extensively applied in laboratory flames and in practical combustion devices [1–4]. The complexity and cost of equipment required for these techniques restricts their use, however, to dedicated laboratory environments. Diode laser technology is increasingly being used for the development of combustion sensors that are compact, inexpensive and robust [5] but the application of such sensors has been almost exclusively restricted to path-integrated absorption measurements, offering little or no information on spatial gradients. Thermometry is possible by wavelength scanning a diode laser over a carefully selected pair of temperature sensitive absorption lines of a species such as, O_2 [6], OH [7], or CO [8]. This and related techniques are appropriate to the study of systems in which the temperature is homogeneous along the beam path; applications have, for example, been demonstrated for thermometry in the combustion chamber of a power plant [9], and in a pulse-detonation engine [10]. Flame temperature measurements have previously been performed by tomographic reconstruction [11], which allows a certain degree of spatial resolution but involves spatial scanning leading to long measurement times, and may struggle to resolve the steep spatial temperature gradients that are present in many flames.

* Corresponding author. Fax: +44 01223 334796.
E-mail address: isb23@cam.ac.uk (I.S. Burns).

1540-7489/$ - see front matter
doi:10.1016/j.proci.2006.07.243

In an effort to address these issues, a wavelength-scanning diode laser technique based on two-line atomic fluorescence (TLAF) was developed previously in our group, which can perform temperature measurements with a spatial resolution that is limited only by the size of the focal spot of the laser beam [12]. Earlier implementations of TLAF had been performed using flashlamps [13] or dye-lasers [14] as the excitation source. The strategy is based on the seeding of trace levels of indium atoms to the flame. Due to the high oscillator strength of atoms, strong fluorescence signals are obtained even when probed with low power diode laser excitation sources. The TLAF technique works by probing the relative populations of two spin-orbit split sub-levels of the indium ground state. It involves the use of two blue diode lasers, emitting at wavelengths of 410.2 and 451.1 nm. Despite the potential and advantages of this approach, one disadvantage is that two laser sources, two filter sets, and two detectors are usually required, as is the case with most other ratiometric techniques. During this research, however, the influence of temperature on the indium fluorescence lineshapes was apparent. The $5^2P_{1/2} \rightarrow 6^2S_{1/2}$ transition at around 410.2 nm has especially good sensitivity as a result of the separation of the hyperfine components; the reason for this will be discussed in more detail below. It was therefore possible to develop a thermometry technique requiring only a single diode laser. Instead of probing the relative intensity of two transitions, it involves probing only one transition, and obtaining temperature information from the spectral lineshape. We call this technique OLAF (one-line atomic fluorescence) to distinguish it from the conventional TLAF approach.

Lineshape-based temperature measurements have been used in *low pressure* environments because, under these conditions, collisional broadening is negligible and the transition width is determined solely by Doppler broadening, whose temperature dependence is governed by a simple relationship. For example, Scheibner et al. [15] used the line-width of absorption spectra of aluminium atoms, acquired using a blue extended cavity diode laser, to determine the temperature in a hollow-cathode lamp, as a function of discharge current. At the conditions of an atmospheric pressure flame, however, the situation becomes more complicated because the lineshape is a convolution of the Doppler profile with a Lorentzian profile, which results from collisional broadening. This makes it considerably more difficult to determine the relationship between the transition width and temperature. Nevertheless, path-averaged flame thermometry based on lineshape analysis has been attempted previously by Sanders et al. [16,17], who seeded caesium atoms to a pulse detonation engine. They derived an empirical value for an exponential coefficient relating the width of the Lorentzian component of the absorbance linewidth ($\Delta\nu_L$) to temperature, and thus obtained good agreement with other measurements of the temporal evolution of temperature in the engine. However, in addition to being a function of temperature, $\Delta\nu_L$ is also dependent on the mole fractions of the species colliding with the probed atom (which may vary spatially and temporally). In estimating the relationship between $\Delta\nu_L$ and temperature, it is consequently important to avoid making a calibration that inadvertently takes into account the effects of varying gas composition. For the LIF technique we propose here, the dependence of $\Delta\nu_L$ on T and on species concentration is explored explicitly using model assumptions that are physically reasonable for the flame conditions that we probe.

The paper begins by briefly outlining the relevant theory of collisional line-broadening, and by drawing attention to the particular advantage of indium as a probe species. This is followed by a description of the experimental set-up required to perform OLAF. Finally, results from measurements performed in a laminar reference flame are presented and the accuracy of the technique is assessed by comparison to CARS, to Na-line reversal, and to numerical simulation performed for identical conditions. The results are discussed before concluding with an overview of the future prospects for the technique.

2. Theory

A short description is given here of the physical mechanisms that lead to the broadening of spectral lines. First, there is Doppler broadening, in which a Gaussian lineshape results from the distribution of molecular velocities in the gas. The full-width-at-half-maximum-height (FWHM) of the Doppler component of the spectral width is defined as:

$$\Delta\nu_D = \frac{2\nu_0}{c}\sqrt{\frac{2(\ln 2)kT}{m}} \tag{1}$$

Here, ν_0 is the transition centre frequency, c is the speed of light in a vacuum, k is the Boltzmann constant, T is the temperature, and m is the molar mass of the probed species. At flame conditions, a broadening resulting from a second mechanism, pressure (or collisional) broadening, is of comparable magnitude and has a Lorentzian lineshape:

$$g_L(\nu) = \frac{\Delta\nu_L}{2\pi}\frac{1}{(\nu-\nu_0)^2 + \left(\frac{\Delta\nu_L}{2}\right)^2} \tag{2}$$

Here, $\Delta\nu_L$ is the FWHM of the Lorentzian profile. The composite spectral shape that results from these effects is defined by the convolution of the

Gaussian and Lorentzian functions, which results in a Voigt profile [18].

As noted above, the functional relationship between the $\Delta\nu_L$ and T is fairly complicated. Nevertheless, an approximate analysis can be made on the basis of certain assumptions. Since, at flame conditions, natural broadening is negligible compared to collisional broadening, the total Lorentzian width can be expressed as the sum of that resulting from adiabatic collisions ($\Delta\nu_{L''}$) and that resulting from non-adiabatic collisions ($\Delta\nu_{L'}$) [19]. The distinction between these is that non-adiabatic collisions result in a change in the energy state of the atom, whereas adiabatic collisions do not. The magnitude of $\Delta\nu_{L'}$ for atoms cannot easily be estimated from theory, but, at flame conditions, is typically an order of magnitude smaller than $\Delta\nu_{L''}$; therefore, in this analysis, the former will be neglected. A further assumption that can be made is the impact broadening approximation [20], by which it is supposed that the duration of collisions between the atom and the broadening partner is insignificant by comparison to the time between collisions. This assumption is valid at the conditions being probed here, and only breaks down at much higher pressure. The radiation that is emitted during collisions can thus be neglected, and the collisions can be regarded as instantaneous. It follows that the only consequence of the collisions is in a phase shift to the emitted radiation. The magnitude of this phase shift depends on the interaction potential between the probed atom and perturbing molecule, which can be approximated by the first term of the van der Waals function [19]:

$$V_{vdw}(R) = \frac{C_6}{R^6} \tag{3}$$

where C_6 is the van der Waals constant and R is the separation between the indium atom and the perturbing particle. From these assumptions, it can be shown that the Lorentzian width is described by:

$$\Delta\nu_L \propto \Delta C_6^{\frac{2}{5}} u^{\frac{3}{5}} N \tag{4}$$

where N is the total number density, ΔC_6 is the difference between the van der Waals constants for the ground and excited states of the absorbing atom, and u is the relative mean velocity between the probed atoms and perturbing molecules,

$$u = \sqrt{\frac{8RT}{\pi\mu}} \tag{5}$$

where μ is the reduced mass, and R is the Universal Gas Constant. Nefedov et al. describe a method for estimating the C_6 interaction potential [19], from which it is apparent that this term is not a function of temperature. If we assume ideal gas behaviour, then $N \propto T^{-1}$, from which it follows that: $\Delta\nu_L \propto T^{-0.7}$, and this is the relationship that will be used throughout this paper. It should be noted that $\Delta\nu_L$ is a function of composition but this dependence will be neglected here since the flames in this study are composed mainly of N_2, which means that mole fractions of other species change much less as a function of flame-stoichiometry or of height-above-burner than in the case of flames without an inert diluent; the validity of this assumption will be discussed in a later section.

Another aspect of theoretical background that it is worthwhile to consider is the reason for selecting indium as the tracer species. In order to reveal the rationale behind this choice, it is instructive to consider the variation in the spectral shape of the indium $5^2P_{1/2} \rightarrow 6^2S_{1/2}$ transition (near 410.2 nm) as a function of temperature. The transition consists of four hyperfine components, the middle two of which lie close to each other, resulting, at flame conditions, in a structure with three separate peaks. Examples of theoretical spectra are shown in Fig. 1: each one represents the sum of four Voigt profiles. The positions and relative intensities of the hyperfine components of the transition are also shown. In Fig. 1a, a base case spectrum has been plotted with Lorentzian width equal to that measured at 2200 K (corresponding to the temperature obtained from a reference measurement, as will be described in a later section); the Doppler width was calculated for the same temperature. Another spectrum is also shown, corresponding to a temperature of 1950 K; in this case, $\Delta\nu_L$ and $\Delta\nu_D$ were calculated from the relationships shown above. Note that in the latter case, the depth of the troughs in the spectrum is less profound. An expanded view of the shaded region in Fig. 1a is shown in b, where four further spectra are shown, separated by intervals of 50 K. The spectra have each been normalised to a maximum value of 1.0 arbitrary units. It is apparent from the figure that the depth of the troughs of the spectrum is very sensitive to temperature. Therefore, the choice of a transition system with several appropriately spaced lines allows for greater temperature sensitivity than would be possible with a single hyperfine line, where the location of the line flanks would need to be determined very accurately. The fidelity of the indium LIF spectra obtained during this study, and the corresponding quality of the spectral fits mean that the technique is sensitive even to small changes around typical flame temperatures.

3. Experiment

The widely tunable extended cavity diode laser, operating around 410.2 nm, which was used during this work, has been described in detail previously [21]. Due to the wide mode-hop free tuning range of this laser system, it was possible

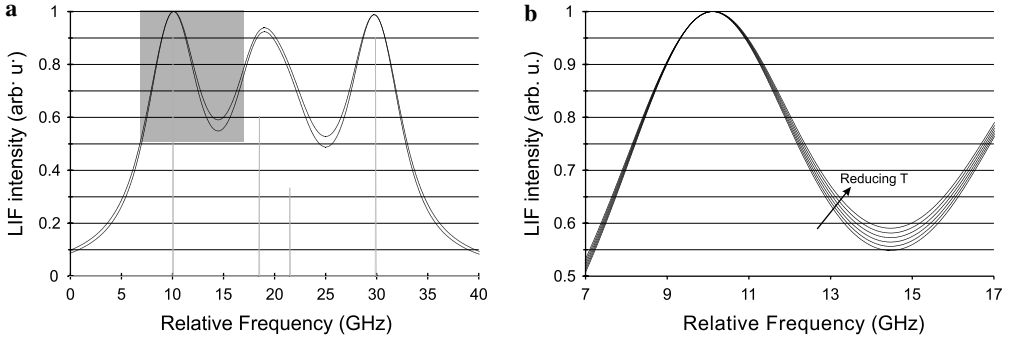

Fig. 1. (a) Simulated indium spectra corresponding to temperatures of 1950 K (shallower troughs) and of 2200 K. The positions of the hyperfine lines are indicated. (b) The shaded region of (a) is shown on an expanded scale, and additional spectra are shown at 50 K intervals, ranging from 1950 to 2200 K.

to perform mode hop-free scanning over the entire $5^2P_{1/2} \rightarrow 6^2S_{1/2}$ transition structure. The laser wavelength scans were performed at a rate of 20 Hz, and the laser power decreased from approximately 1.4 to 0.8 mW during the scan, due to tuning of the injection current. The experimental set-up for the thermometry experiment is shown in Fig. 2. The output beam of the extended cavity diode laser was focussed ($f = 300$ mm) to a beam diameter of around 100 μm on the centreline of an axis-symmetric flame. The burner was mounted on a translation stage which allowed for the adjustment of its height. Prior to passing through the flame, part of the laser beam was reflected by a glass plate towards a quartz etalon (FSR = 3.00 GHz); the transmitted fringe pattern of this etalon was used to ensure that the laser scans were mode-hop free, and also made it possible to compensate for slight non-linearities in the wavelength scanning rate. A second glass plate was used to reflect part of the laser beam to a photodiode as a reference power measurement, which was used to normalise the fluorescence intensity. Another photodiode was used to measure the power of the laser beam after passing through the flame, allowing the absorbance spectrum to be evaluated. The fluorescence signal was imaged at $f/\# = 2.4$ through a pin-hole ($d = 500$ μm) and an interference filter centred around 451.1 nm (CVI, $\Delta\lambda = 3$ nm) onto a photomultiplier tube (Hamamatsu, R3788); the photomultiplier signal was pre-amplified (gain = 10^5; bandwidth = 20 kHz). This resulted in a measurement volume defined by a cylinder with a diameter of 0.1 mm and length of 0.5 mm. The detection of non-resonant fluorescence in the $5^2P_{3/2} \rightarrow 6^2S_{1/2}$ transition, at around 451.1 nm, avoided any interference that could otherwise have resulted from scattered laser light from the surface of the burner plate. The electronic signals were digitised using an oscilloscope, and the averages of 128 individual wavelength scans were stored. Measurements of the background readings were taken and were subtracted from the experimental data. It has previously been confirmed that for laser irradiances such as those used here, the fluorescence intensity is a linear function of laser power [12].

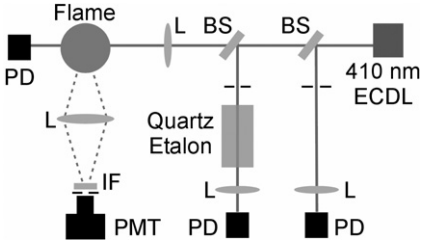

Fig. 2. The experimental set-up for the OLAF thermometry experiments (L, lens; IF, interference filter centred around 451.1 nm; PMT, photomultiplier tube; PD, photodiode; BS, beamsplitter; ECDL, extended cavity diode laser).

A one-dimensional laminar flame of CH_4 and air was stabilised on a custom-designed Mèker-type burner. The burner consisted of a metal plate with drilled holes ($d = 0.5$ mm; spacing = 0.25 mm) resulting in a flat flame-front located approximately 1 mm above the burner surface. The flame was seeded by passing a portion of the air stream through a nebuliser containing an aqueous solution of $InCl_3$ (~0.05 M), which resulted in a concentration of indium atoms in the flame of approximately 100 ppb. This tiny seeding concentration was not observed to cause any perturbation to the flame properties. An unseeded co-flow flame ($d = 60$ mm) was present, and was run at the same stoichiometry as the inner seeded flame ($d = 40$ mm), which meant that the seeded region was homogeneous in temperature, thus allowing accurate path-integrated temperature measurements to be performed by the Na-line reversal technique, for the purpose of

comparison. Reference temperature measurements were made, at precisely the same flow conditions, by Na-line reversal, and by vibrational coherent anti-Stokes Raman scattering (CARS) of N_2. Details of the burner and of its characterisation by CARS, Na-line reversal, and numerical simulation are presented elsewhere [22]. It should be noted that this flame geometry was selected for the purpose of the Na-line reversal technique: the OLAF diode laser thermometry tool presented here is expected to work equally well in other flame configurations.

Due to the long path length and flat flame front of the burner used during these experiments, there was non-negligible absorption of the laser beam by atomic indium as it passed through the flame (typically around 10%). The same experiments could readily have been performed with considerably lower concentrations of seeded indium, thus avoiding this laser absorption, since the acquired spectra are far from being shot-noise limited, as discussed further below. The absorption of the laser beam could be thoroughly compensated for because of the homogeneity of the flame, which allowed the laser power at the measurement volume to be determined with accuracy. Signal trapping did not influence the lineshape of the acquired spectra, since we perform here an excitation scan, and perform broadband detection; the proportion of the fluorescence being absorbed is thus independent of the excitation wavelength. Spectra were taken at a range of stoichiometries at 12 mm height above burner (HAB), and at a range of heights above the burner for $\phi = 1.0$.

Theoretical spectra comprising the sum of four Voigt profiles were fitted to the experimental data for each of the flames conditions studied. In the case of both the ϕ scan and the height scan, the case of $\phi = 1.0$ and HAB = 12 mm was used as a calibration point. In fitting the spectrum for this point, $\Delta\nu_D$ was fixed to a value of 2.3 GHz, which was calculated for a temperature of $T_{ref} = 2200$ K (measured at the same conditions by the Na-line reversal method). The relative spectral positions and relative intensities of the four hyperfine lines are well known. The four fitted parameters were: the spectral location and intensity of the leftmost hyperfine component; the Lorentzian width ($\Delta\nu_L$); and the intensity of background radiation. This resulted in a reference Lorentzian width of $\Delta\nu_L^{ref} = 5.01$ GHz. The calibration therefore allowed a relationship to be developed for $\Delta\nu_L$ at other temperatures:

$$\Delta\nu_L = \Delta\nu_L^{ref}\left(\frac{T^{ref}}{T}\right)^{0.7} \quad (6)$$

Thus for the rest of the measurements, T was a fitted parameter and $\Delta\nu_L$ and $\Delta\nu_D$ were related by Eqs. (1) and (6) to T. The resulting temperature data are presented and discussed in the following section. This type of calibration is likely to be valid for any hydrocarbon–air flame burned at atmospheric pressure.

4. Results and discussion

Figure 3 shows an example of a fluorescence spectrum with a fitted spectrum superimposed. It is clear from the small residual that there is a very close agreement between the theoretical spectrum and the experimental data. For this reason, the fitted spectra allow an accurate evaluation of the Lorentzian width of the transitions.

Figure 4 shows the results of the stoichiometry scan in the flat-flame burner. The graph to the left shows the measured OLAF temperature (T_{line}) as a function of ϕ at HAB = 12 mm. The results of reference measurements performed with Na-line reversal (T_{Na}), and of numerical calculations using PREMIX [23], are also shown as a comparison. It can be seen that there is good agreement between the results of the two experimental techniques. The theoretical maximum error of the Na-line reversal experiment has been estimated to be ±15 K. A further error of a similar magnitude results from the limited precision with which the gas flowrates can be reproduced. There is agreement between T_{line} and T_{Na} to within 6% at all stoichiometries, and the model results also concur with the experimental data. The graph to the right of Fig. 4 shows the relationship of the fitted Lorentzian width to ϕ. The value of $\Delta\nu_L$ that would be expected from T_{Na}, using Eq. (6), is also shown. This plot reveals that the model for temperature dependence of $\Delta\nu_L$ does not give perfect

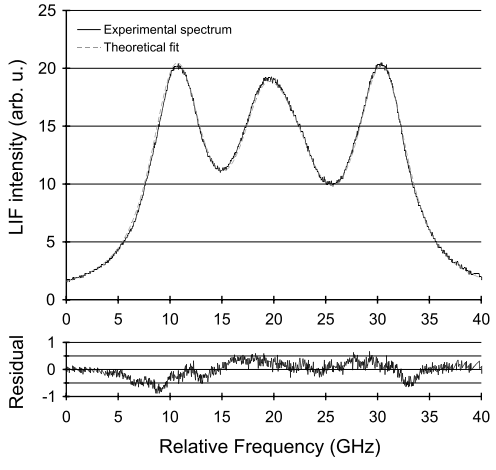

Fig. 3. The average of 128 indium fluorescence spectra is shown along with a theoretical fitted spectrum. The residual between the experimental and fitted spectra is shown on a separate axis.

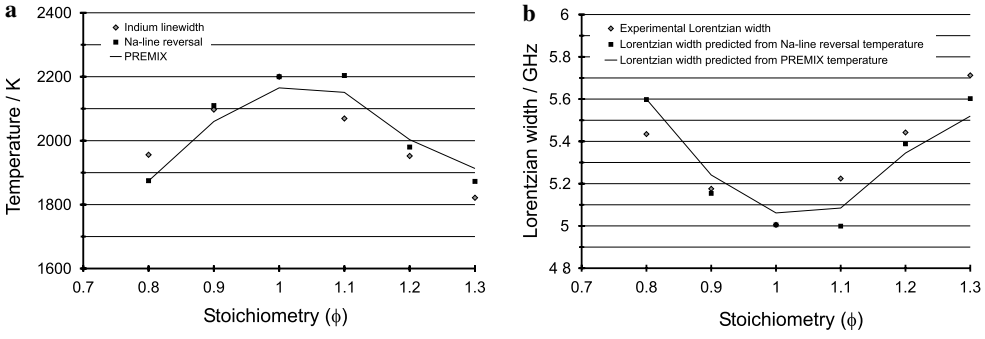

Fig. 4. (a) Measured flame temperatures at 12 mm HAB as a function of ϕ. The linewidth temperature at $\phi = 1.0$ was fixed to the value measured by Na-line reversal, and the temperatures for the other points were calculated from Eq. (6). Temperatures measured by Na-line reversal in the same burner, and the results of calculations with the PREMIX code [23], are shown for comparison. (b) Fitted Lorentzian widths of the indium spectra as a function of ϕ, and Lorentzian widths predicted from the Na-line reversal temperature measurements at the same conditions.

agreement with the experimental data. This may result from a combination of several factors. First, the true exponent describing the relationship between $\Delta\nu_L$ and T may differ from the predicted value of 0.7. This could result from the influence of non-adiabatic collisions, or from adiabatic collisions that are not well described by the impact approximation and the use of the C_6 potential. Alternatively, the dependence of $\Delta\nu_L$ on T may be correctly described by the exponential coefficient of 0.7, but there may be a weak influence of composition on $\Delta\nu_L$. For adiabatic collisions with molecules described by the C_6 potential, $\Delta\nu_L$ is directly proportional to the polarizability, α, of the colliding partner, and is related through Eq. (4) to the relative mean velocity. It is thus possible to estimate the expected variation in $\Delta\nu_L$ over the stoichiometry range studied here ($\phi = 0.8$–1.3). Based on simulated major species composition, using PREMIX, and available polarizability data [24] the maximum change in $\Delta\nu_L$ would be 0.6% over the range covered in Fig. 4. This would translate into a systematic error in evaluated temperatures of around 15 K.

Since the species that differs most from N_2 in its properties as a broadening partner is H_2O, it is anticipated that any such effects of flame-stoichiometry on $\Delta\nu_L$ would probably be somewhat less significant for other types of hydrocarbon–air flames: for hydrocarbon fuels other than methane, the C:H ratio is higher so the mole fraction of H_2O in the product gases would be lower. Similarly, in turbulent flames in which ambient air is entrained in the flow, the mole fraction of N_2 increases, thereby reducing the influence of flame-stoichiometry on $\Delta\nu_L$. Despite this, it is also possible that a significant part of the deviation between T_{line} and T_{Na} may simply be caused by stochastic scatter of the data resulting from an error in the estimation of $\Delta\nu_L$ from the experimental spectra.

Such scatter is clearly evident in Fig. 5, which shows the results of a height scan in the flame. There is very little composition change as a function of HAB, and the temperature gradient is only significant close to the surface of the burner plate. The temperature was measured by Na-line reversal only at HAB = 12 mm. Therefore, the results of CARS temperature measurements performed at the same conditions, and of a model performed using the PREMIX code, are also shown in Fig. 5. The CARS measurements represent averages of temperatures obtained by theoretical fits to 600 individual experimental spectra with an estimated accuracy of ±40 K. It is clear that the line-width measurements correctly follow the trend in fairly sharp temperature increase in the region just above the flame front, which results from the slow exothermic reaction of CO to form CO_2. This is followed by a gentle increase above about

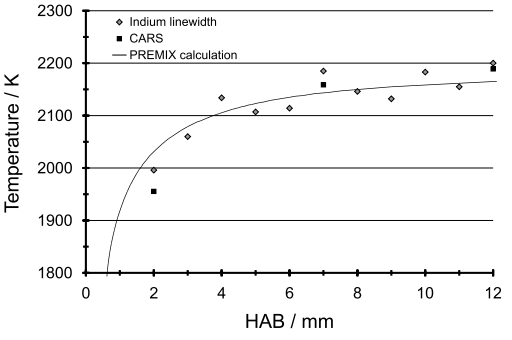

Fig. 5. Measured temperature as a function of height above burner (HAB) for stoichiometry $\phi = 1.0$. The linewidth temperature scale is locked to the value measured by Na-line reversal at HAB = 12 mm. Temperature measurements by CARS, and the results of calculations from the PREMIX code [23], are also shown.

HAB = 4 mm. By comparing T_{line} to the model results, it is evident that the T_{line} data are scattered by approximately ±40 K around the mean, which can only be attributed to random error.

The results reported here represent the first spatially resolved measurements of flame temperature using a single diode laser. Future development could be directed toward the possibility of much faster measurements, since thermometry in dynamic systems requires both high temporal and spatial resolution. Although high-quality averaged spectra were analysed for illustrative purposes during this study, it is emphasised that the spectra were far from being shot-noise limited, so the latter does not constitute a limitation to measurement speed. From the signal strength and detector characteristics, it has been estimated that a signal to noise ratio of around 20 would be possible for a spectrum recorded in as short a time as 100 μs with exactly the same equipment as used during the present study. The measurement speed could therefore be increased substantially without loss of precision. It is clear that a further requirement for a high-speed temperature measurement would be a substantially increased laser wavelength tuning rate. In this context, it should be noted that recent developments in extended cavity diode laser technology open the possibility of wavelength tuning at kHz scanning rates [25].

5. Conclusions

This paper has described the development of a novel flame temperature measurement technique based on the analysis of the lineshapes of fluorescence spectra of atomic indium. The spectra were generated using a single diode laser and this technique therefore offers the advantage of greater simplicity by comparison to multi-laser diagnostics, while retaining favourable aspects such as spatial resolution and accuracy. Atomic indium was chosen as the probe species due to the sensitivity of the spectral shape to temperature at flame conditions. A theoretical model was employed to describe the relationship of T with $\Delta\nu_L$, instead of forcing the predicted temperature to agree with the reference measurements by introducing an empirical calibration constant. The measurements of temperature by the single-diode laser OLAF technique have been carefully compared to accurate reference measurements in a one-dimensional laminar flame that was stabilised on a burner allowing seeding of metal atoms. The OLAF results show good agreement with the expected temperatures but possible reasons for small discrepancies have been highlighted. The technique is accurate, inexpensive, and simple to implement, and, combined with independent pressure measurements, conducted simultaneously, has the potential even for measurements in environments where the pressure fluctuates. This diode-laser-induced fluorescence technique has potential for application in sooting flames, where other thermometry methods such as CARS and spontaneous Raman scattering are subject to interferences. Faster laser-scanning rates may in future allow this technique to be used for the study of dynamic flame behaviour.

Acknowledgments

This work was supported by grants from the Paul Instrument Fund of the Royal Society. I.S.B. is grateful to St. John's College, Cambridge for a Research Fellowship. J.H. was supported by an Advanced Research Fellowship from the EPSRC. C.F.K. is thankful to the EPSRC for the provision of a PLATFORM grant and to the Leverhulme trust for sponsorship.

References

[1] A.C. Eckbreth, *Laser Diagnostics for Combustion Temperature and Species*, Second ed., Gordon and Breach, Amsterdam, 1996.
[2] N.M. Laurendeau, *Prog. Energy Combust. Sci.* 14 (1988) 147–170.
[3] W.P. Stricker, in: K. Kohse-Höinghaus, J.B. Jeffries (Eds.), *Applied Combustion Diagnostics*, Taylor and Francis, New York, 2002, pp. 155–193.
[4] J.W. Daily, *Prog. Energy Combust. Sci.* 23 (1997) 133–199.
[5] M.G. Allen, *Meas. Sci. Technol.* 9 (1998) 542–562.
[6] S.T. Sanders, J. Wang, J.B. Jeffries, R.K. Hanson, *Appl. Opt.* 40 (2001) 4404–4415.
[7] T. Aizawa, *Appl. Opt.* 40 (2001) 4894–4903.
[8] J.H. Miller, S. Elreedy, B. Ahvazi, F. Woldu, P. Hassanzadeh, *Appl. Opt.* 32 (1993) 6082–6089.
[9] H. Teichert, T. Fernholz, V. Ebert, *Appl. Opt.* 42 (2003) 2043–2051.
[10] L. Ma, S.T. Sanders, J.B. Jeffries, R.K. Hanson, *Proc. Combust. Inst.* 29 (2002) 161–166.
[11] R. Villarreal, P.L. Varghese, *Appl. Opt.* 44 (2005) 6786–6795.
[12] J. Hult, I.S. Burns, C.F. Kaminski, *Proc. Combust. Inst.* 30 (2005) 1535–1543.
[13] N. Omenetto, P. Benetti, G. Rossi, *Spectrochim. Acta, B* 27 (1972) 453–461.
[14] J.E. Dec, J.O. Keller, *Proc. Combust. Inst.* 21 (1986) 1737–1745.
[15] H. Scheibner, S. Franke, S. Solyman, J.F. Behnke, C. Wilke, A. Dinklage, *Rev. Sci. Instrum.* 73 (2002) 378–382.
[16] S.T. Sanders, D.W. Mattison, L. Ma, J.B. Jeffries, R.K. Hanson, *Opt. Exp.* 10 (2002) 505–514.
[17] S.T. Sanders, D.W. Mattison, J.B. Jeffries, R.K. Hanson, *Proc. Combust. Inst.* 29 (2002) 2661–2667.
[18] W. Demtröder, *Laser Spectroscopy*, Third ed., Springer-Verlag, Berlin, 2003.
[19] A.P. Nefedov, V.A. Sinel'shchikov, A.D. Usachev, *Phys. Scr.* 59 (1999) 432–442.

[20] I.I. Sobelman, L.A. Vainshtein, E.A. Yukov, *Excitation of Atoms and Broadening of Spectral Lines*, Springer-Verlag, Berlin, 1981.
[21] J. Hult, I.S. Burns, C.F. Kaminski, *Appl. Opt.* 44 (2005) 3675–3685.
[22] G. Hartung, J. Hult, C.F. Kaminski, *Meas. Sci. Technol.* (2006) in press.
[23] R.J. Kee, J.F. Grcar, M.D. Smooke, J.A. Miller, Report No. SAND85-8240, Sandia National Laboratories, 1993.
[24] D.R. Lide (Ed.), *CRC Handbook of Chemistry and Physics*, Seventy-seventh ed., CRC Press, Boca Raton, USA, 1996.
[25] L. Levin, *Opt. Lett.* 27 (2002) 237–239.

Comments

Alan Eckbreth, Consultant, USA. Given that the temperature measurements are based on the depth of the troughs, an accurate determination of the zero base-line would seem to be important. How would fluorescent or background luminosity interferences affect your measurement accuracy?

Reply. Each temperature measurement was performed by fitting a theoretical spectrum to the experimental results, thus exploiting the sensitivity of the full spectral shapes. Sensitivity exists due to the relative change of the trough depths to peak heights as temperature varies. There were four variable parameters in the fitting process, one of which was a dc background intensity stemming from flame emission and seeder species chemiluminescence. High quality fits were only obtained when the background was correctly accounted for. The high fidelity of the recorded spectra allows both the temperature and the background offset to be determined with accuracy.

•

Scott Sanders, University of Wisconsin Madison, USA. How generally applicable is lineshape-based thermometry in combustion systems? What is the sensitivity of the inferred temperature to gas pressure? If I try to apply your technique to a different atmospheric—pressure combustor, will I need to recalibrate using Na-line reversal or similar?

Reply. This thermometry technique is likely to be applicable in any air–hydrocarbon combustion occurring at or below atmospheric pressure, although it should be noted that the gas pressure must be known in order to determine the temperature accurately. We believe that the type of calibration described here is suitable for use in other air–hydrocarbon flames at atmospheric pressure, and that repeated recalibration should not be required.

•

Volker Sick, The University of Michigan, USA. What are the accuracy and precision limits for measured temperatures?

Reply. A conservative estimate of the accuracy may be made by comparing the temperatures derived from the indium fluorescence lineshape to the reference measurements and to the modeling results: the largest deviation is around 6%. This figure certainly overestimates the uncertainty introduced by the one-line atomic fluorescence technique because there are non-negligible errors in the reference measurements and in the modeling. There are further contributions from possible changes in the flame conditions since the reference measurements were not performed simultaneously to the OLAF measurements. A recent paper describing the burner used during these experiments [1] gives details of limitations on how accurately the gas flow rates can be controlled, leading to a slight but appreciable contribution to the temperature uncertainty.

The precision of the measurements may be approximated by considering the height scan data shown in Fig. 5. In the region of roughly constant temperature between 4 and 12 mm above the burner, the deviations between the measured temperature and the modeling results are of a magnitude of $\pm 1.3\%$. The true precision is better than this though, since this number also includes, for example, the effect of small fluctuations in the gas flowrates during the experiment.

Reference

[1] G. Hartung, J. Hult, C.F. Kaminski, *Meas. Sci. Tech.* 17 (2006) 2485–2493.